©ESO 2020

LETTER TO THE EDITOR

# *Chandra*'s X-ray study confirms that the magnetic standard Ap star KQ Vel hosts a neutron star companion[*]

Lidia M. Oskinova[1, 2], Richard Ignace[3], Paolo Leto[4], and Konstantin A. Postnov[5, 2]

[1] Institute for Physics and Astronomy, University Potsdam, D-14476 Potsdam, Germany
[2] Department of Astronomy, Kazan Federal University, Kremlevskaya Str 18, Kazan, Russia
[3] Department of Physics & Astronomy, East Tennessee State University, Johnson City, TN, 37614, USA
[4] NAF - Osservatorio Astrofisico di Catania, Via S. Sofia 78, I-95123 Catania, Italy
[5] Sternberg Astronomical Institute, M.V. Lomonosov Moscow University, Universitetskij pr. 13, 119234 Moscow, Russia

## ABSTRACT

*Context.* KQ Vel is a peculiar A0p star with a strong surface magnetic field of about 7.5 kG. It has a slow rotational period of nearly 8 years. Bailey et al. (2015) detected a binary companion of uncertain nature, and suggested it could be a neutron star or a black hole.
*Aims.* We analyze X-ray data obtained by the *Chandra* telescope to ascertain information about the stellar magnetic field and/or interaction between the star and its companion.
*Methods.* We confirm previous X-ray detections of KQ Vel with a relatively large X-ray luminosity of $2 \times 10^{30}$ erg s$^{-1}$. X-ray spectra suggest the presence of hot gas at > 20 MK and, possibly, of a non-thermal component. X-ray light curves are variable, but better quality data are needed to determine periodicity if any.
*Results.* We interpret X-ray spectra as a combination of two components: the non-thermal emission arising from the aurora on the A0p star and the hot thermal plasma filling the extended shell surrounding the "propelling" neutron star.
*Conclusions.* We explore various alternatives, but a hybrid model involving the stellar magnetosphere along with a hot shell around the propelling neutron star seems most plausible. We speculate that KQ Vel was originally a triple system, and the Ap star is a merger product. We conclude that KQ Vel is an intermediate-mass binary consisting of a strongly magnetic main sequence star and a neutron star.

**Key words.** Stars: early-type — Stars: individual: KQ Vel — Stars: magnetic — Stars: massive — X-rays: stars

## 1. Introduction

KQ Vel (HD 94660, HR 4263) is a nearby star at $d \approx 114$ pc with a long history of study. It was first identified as a chemically peculiar A star by Jaschek & Jaschek (1959), while strong surface magnetic field was detected by Borra & Landstreet (1975). The current estimates show that the field strength is in excess of 7.5 kG (e.g., Mathys 2017). The star is an exceedingly slow rotator, with a rotation period of about 2800 d (Table 1).

Bailey et al. (2015) determined that the star has a complex magnetic field, strongly non-solar abundances, with large over-abundance of Fe-peak and rare-earth elements, and shows remarkable radial velocity variations with a period ∼ 840 d. The binary companion is not seen in optical, which led Bailey et al. (2015) to suggest the first detection of a compact companion with mass ≳ 2 $M_\odot$ for a main sequence magnetic star.

Among all A-type stars so far detected in X-rays, KQ Vel is the second most X-ray luminous (Robrade 2016). The record holder is KW Aur, where very soft X-ray emission likely arises from a white dwarf companion (Schröder & Schmitt 2007). This begs the question of whether the exceptional X-ray production from KQ Vel also arises from its compact companion. In addition, a popular model for explaining X-ray emissions from magnetic stars is the magnetically confined wind shock (MCWS)

model of Babel & Montmerle (1997). This model has been developed to explain X-ray emissions from the magnetic A0P star IQ Aur, however it fails to explain why some magnetic Ap stars are X-ray dim (Robrade 2016). The MCWS model requires the presence of radiatively driven stellar winds. Very little is known about the winds of non-supergiant A stars (Babel 1996; Krtička et al. 2019). What is clear, however, that the winds of these stars are very weak.

Recently, radio studies of strongly magnetic chemically peculiar Bp stars revealed variable polarimetric behavior and radio continua consistent with non-thermal processes resulting from auroral mechanisms (e.g., Leto et al. 2017, 2018, 2020). Robrade et al. (2018) suggested that the auroral mechanisms operates also in strongly magnetic Ap stars, such as CU Vir, which is detected in X-rays with $L_X \approx 3 \times 10^{28}$ erg s$^{-1}$ and has hard X-ray emissions with $T_X \approx 25$ K.

We undertook a study of the X-ray emission from KQ Vel measured by the *Chandra* X-ray telescope to clarify its origin: could the emission arise from (a) the compact companion, (b) the star's magnetosphere, or (c) an interaction between the weak but magnetized wind of KQ Vel and its compact companion. In section 2 we describe the new X-ray data. A discussion of the results is given in section 3 toward resolving the origin of the X-rays. Section 4 presents concluding remarks, while detailed model calculations are presented in Appendix.

---

[*] The scientific results reported in this article are based on observations made by the *Chandra* X-ray Observatory (ObsID 17745).

**Table 1.** Stellar Properties of KQ Vel[*]

| Sp. Type | A0p EuSiCr |
|---|---|
| Distance | 114 pc |
| Temperature | 11 300 K |
| Radius | 2.53 $R_\odot$ |
| Luminosity, $L_{bol}$ | $3.5 \times 10^{35}$ erg s$^{-1}$ |
| Mass | $3.0 \pm 0.2\ M_\odot$ |
| Magnetic field strength | 7500 G |
| Rotation period, $P_{rot}$ | 2800 d |
| Orbital period, $P_{orb}$ | 840 d |
| Eccentricity, $e$ | 0.36 |

[*] from Bailey et al. (2015) and references therein

## 2. X-ray properties of KQ Vel

### 2.1. X-ray spectra

KQ Vel was observed by the ACIS-I instrument on board the *Chandra* X-ray telescope on 2016-08-20 for 25 ks (ObsID 17745). We retrieved and analyzed these archival X-ray data using the most recent calibration files. The spectrum and the light curve were extracted using standard procedures from a region with diameter ≈ 7″. The background area was chosen in a nearby area free of X-ray sources. The net count rate is 0.1 s$^{-1}$. The pile-up is ≈ 13% and does not significantly affect the spectral fitting results. Throughout the text, the X-ray properties of KQ Vel are reported in the 0.3–11.0 keV band.

To analyze the spectra we used the standard X-ray spectral fitting software xspec (Arnaud 1996). The abundances were scaled relative to solar values according to Asplund et al. (2009). KQ Vel is a chemically peculiar star. For example, Bailey et al. (2015) find overabundances among the iron group elements by factors of 1000. However allowing for non-solar abundances during spectral fitting does not improve the fits of these low-spectral resolution data, and for now we adopt solar abundances.

Spectral fits of similar statistical quality were obtained using two different spectral models: (1) purely thermal plasma model with a two-temperature (2T) collisional ionization equilibrium (*apec*) components, with the hottest plasma at ≈ 30 MK; (2) combined thermal and non-thermal model which assumed a thermal, *apec*, component plus a power-law (see Fig. 1). In this spectral model, the thermal plasma component has a temperature of ≈ 10 MK. The parameters of best fit models are listed in Table 2.

For both models, when the newest calibration files that account for the contamination on the ACIS-I detector are used, the neutral hydrogen column density, $N_H$, is consistent with being negligible. Based on Fitzgerald (1970) and Ducati et al. (2001), the intrinsic color[1] of an A0 star is $(B-V)_0 = -0.08$. The observed $(B-V)_{obs} = 0.02$, formally implying a negative reddening $E(B-V) = (B-V)_{obs} - (B-V)_0$. We interpret this as a very low level of interstellar reddening, and, correspondingly, a low neutral H column density in the direction of KQ Vel; this is consistent with the results from X-ray spectral modeling.

From the Rankine-Hugoniot condition for a strong shock, the post-shock temperature is given by $T \approx 14$ MK $\times (v_w/10^3$ km s$^{-1})^2$, for $v_w$ the wind speed. Achieving a temperature of 30 MK would require the speeds exceeding 1500 km s$^{-1}$. This is significantly larger than expected for A0V stars; e.g. the empirically estimated terminal wind velocities of the main sequence B-type stars do not exceed 1000 km s$^{-1}$ (Prinja 1989).

---

[1] We used tables found at www.stsci.edu/~inr/intrins.html that are based on the work of the cited authors.

**Table 2.** X-ray Spectral Model Fitting

| Thermal model (*tbabs(apec+apec)*) | |
|---|---|
| $kT_1$ | $0.81 \pm 0.04$ keV |
| $EM_1$ | $(3.5 \pm 0.8) \times 10^{52}$ cm$^{-3}$ |
| $kT_2$ | $2.5 \pm 0.2$ keV |
| $EM_2$ | $(7.1 \pm 0.4) \times 10^{52}$ cm$^{-3}$ |
| $\langle kT \rangle \equiv \sum_i kT_i \cdot EM_i / \sum_i EM_i$ | 1.9 keV |
| reduced $\chi^2$ for 95 d.o.f. | 1.1 |
| Flux[a] | $1.3 \times 10^{-12}$ erg cm$^{-2}$ s$^{-1}$ |
| **Thermal plus a power-law model, (*tbabs(apec+power)*)** | |
| $kT$ | $0.88 \pm 0.04$ keV |
| $EM$ | $(3 \pm 0.5) \times 10^{52}$ cm$^{-3}$ |
| $\alpha$ | $2.5 \pm 0.2$ |
| $K$ (at 1 keV) | $(2.4 \pm 0.3) \times 10^{-4}$ keV$^{-1}$ cm$^{-2}$ s$^{-1}$ |
| reduced $\chi^2$ for 95 d.o.f. | 1.1 |
| Flux[a] | $1.5 \times 10^{-12}$ erg cm$^{-2}$ s$^{-1}$ |
| $L_X$[b] | $3 \times 10^{30}$ erg s$^{-1}$ |
| log $L_X/L_{bol}$ | $-5$ |

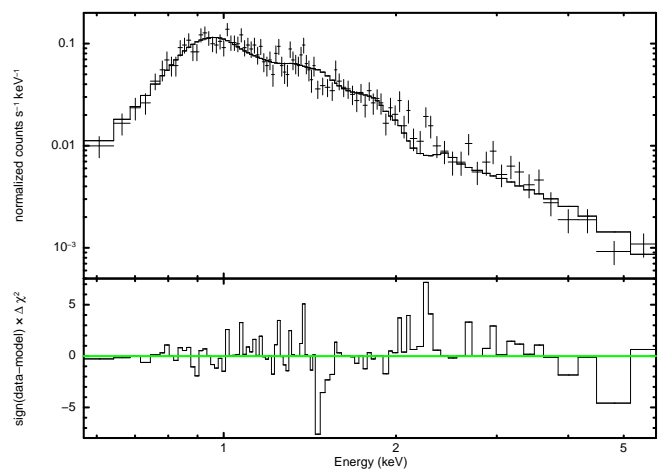[a] observed; in the 0.3–11 keV band



**Fig. 1.** A part of the *Chandra* ACIS-I spectrum of KQ Vel in the 0.5–9 keV energy range and with error bars corresponding to $3\sigma$ is shown by data points. The solid line shows the best fit 2T (*apec*) plus power-law model. The model was fit over the 0.3–11 keV energy band. The model parameters are given in Table 2.

We favor the combined, thermal and non-thermal plasma model as better motivated physically. By analogy with the Bp stars, the non-thermal X-rays in the spectrum of KQ Vel could be explained as bremsstrahlung emission from a non-thermal electron population which are also responsible for the gyro-synchrotron stellar radio emission. When they impact the stellar surface, X-rays are radiated by thick-target bremsstrahlung emission. This physical process is well understood; in particular, the spectral index $\alpha$, of the non-thermal photons, can be related to the spectral index $\delta$, of the non-thermal electron population, by the simple relation $\delta = \alpha + 1$ (Brown 1971). Then, using the best fit X-ray spectrum of KQ Vel, the spectral index of the non-thermal electron energy distribution is $\delta = 3.5$ .

An X-ray light curve of KQ Vel shown in Figure 2 is variable. The power-density spectrum was calculated using a Fourier algorithm (Horne & Baliunas 1986). The largest peak in power
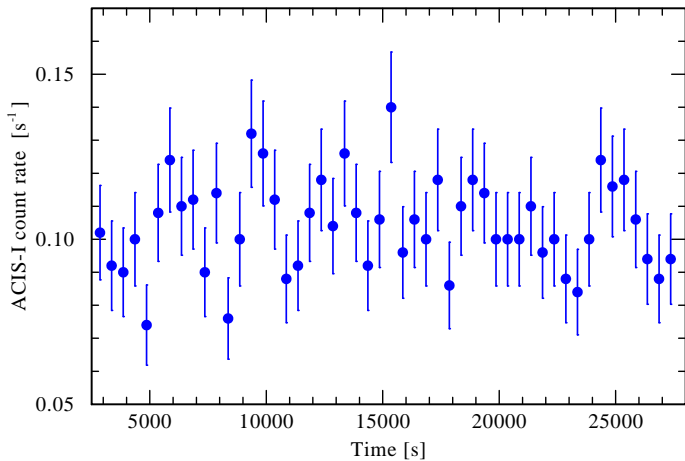
**Fig. 2.** X-ray light curve of KQ Vel. Data are for the 0.3–10.0 keV (1.24–62 Å) energy band, where the background was subtracted. The horizontal axis denotes the time after the beginning of the observation in seconds. The data were binned to 500 s. The vertical axis shows the count rate as measured by the ACIS-I camera. The error bars ($1\sigma$) correspond to the combination of the error in the source counts and the background counts.

density appears at a period of $P_X = 3125 \pm 500$ s, but with a false-alarm probability of 50%. Consequently, the period is not statistically significant. However, the periodicities at amplitudes too low to be detected with the current data cannot be ruled out.

# 3. Discussion

The *Chandra* data reveal that KQ Vel is extraordinary in its X-ray properties – not only this star is among most luminous, it is also the hardest X-ray source among Ap type stars. In the following sections, we explore several different models in an attempt to explain the observed X-ray properties of the KQ Vel: the overall level of X-ray emission, and its hardness and variability.

## 3.1. Auroral X-ray emission of a magnetic Ap star

Recent improvements of MCWS models account for the auroral emission, and are capable of explaining jointly radio and X-ray observations of magnetic B2Vp stars (Leto et al. 2017, 2020).

Auroral model was also successfully applied to the Ap star CU Vir (Robrade et al. 2018). However, there are principal differences between CU Vir and KQ Vel. The former is a fast rotator ($P_{rot} \approx 0.52$ d) whereas the later rotates very slowly ($P_{rot} \approx 2800$ d). Furthermore, the polar field of CU Vir is about two times smaller than for KQ Vel (Kochukhov et al. 2014). A high field strength is a key parameter for accelerating plasma electrons or protons up to relativistic energies. Upon impinging on the stellar surface at the polar caps, this population of non-thermal particles (electrons/protons) radiate non-thermal X-rays by thick target bremsstrahlung. The viewing geometry of KQ Vel is favorable to see always the same stellar magnetic pole (Bailey et al. 2015). On the other hand, stellar rotation has a key role in the generation of the non-thermal electrons. In slow rotators, such as KQ Vel, the centrifugal effect that helps the trapped material to break the magnetic field lines becomes negligible. Therefore, the thermal electrons at the equatorial current sheet have much lower density compared to the case of fast rotation. Indeed, all ApBp stars with detected auroral radio or/and X-ray emission are fast rotators. In the case of the B2V star $\rho$ Oph A,

which has its X-ray emission mainly sustained by auroral mechanism, the ratio between the X-ray and the radio luminosity is $L_X/L_{\nu,\,radio} = 10^{14}$ Hz (Leto et al. 2020). Adopting this ratio, the expected radio luminosity of KQ Vel is at the mJy level.

We believe that the auroral mechanism can be responsible for the non-thermal spectral component in the X-ray spectrum of KQ Vel. However, to explain its thermal X-ray emission, additional mechanisms must be invoked.

## 3.2. Binarity with a non-degenerate companion

KQ Vel is a binary star. The analysis of radial velocity variations by Bailey et al. (2015) suggests a companion of around 2 $M_\odot$. They argue that such a companion could not be an optical star, or spectral features betraying its nature would have been detected. They conclude that the companion is a compact object – either a neutron star (NS) or a black hole (BH). Besides, they consider a possibility of a hierarchical system, perhaps with two lower mass companions in a tighter binary.

In this latter scenario, the unusually hard and luminous X-rays could be coronal in nature, arising either or both of the companions. However, the KQ Vel X-ray luminosity is 3–5 times greater than the star II Peg (Testa et al. 2004) or $\sigma$ Gem (Huenemoerder et al. 2013), which are considered strong coronal sources (D. Huenemoerder, private comm).

The companion could be an active RS CVn type binary consisting of coronal stars. These binaries have typical X-ray luminosities of $10^{30} - 10^{31}$ erg s$^{-1}$ (Walter & Bowyer 1981; Dempsey et al. 1993), i.e. similar to the observed in KQ Vel. Montes et al. (1995) studied the behavior of activity indicators, such as H$\alpha$, Ca II K, and X-ray emission in a sample of 51 chromospherically active binary systems. It was demonstrated that the activity indicators are correlated. Assuming that X-ray luminosity of KQ Vel is due to a hidden RS CVn-type companion, one would expect it contribution to H$\alpha$, H$\epsilon$, and Ca II K lines observed in the KQ Vel spectra. However, Bailey et al. (2015) do not report peculiarities in these lines, especially in Ca II K (see their section 6.5). Hence, for now, we discard a RS CVn companion as a possible explanation for the X-ray emission from KQ Vel's.

Han et al. (2003) performed binary population synthesis that predicted a large population of A0+sdB binary stars. The typical mass of an sdOB star is lower than the companion mass in KQ Vel, moreover the X-ray luminosity of KQ Vel is significantly higher than that of sdOB stars (Mereghetti & La Palombara 2016). At present, we consider this scenario unlikely.

## 3.3. Binary with a degenerate companion

Bailey et al. (2015) proposed that KQ Vel has a NS or a BH companion. An immediate question is whether this could explain the remarkable X-ray emission of KQ Vel.

### 3.3.1. Accreting neutron star, middle age pulsar, or a cataclysmic variable?

The wind mass-loss rate from an A0 star is very small (Babel 1996). An upper limit of $10^{-12}$ $M_\odot$ yr$^{-1}$ has been determined for CU Vir (Krtička et al. 2019), which has the same spectral type as KQ Vel. From spindown considerations, using equation (25) from Ud-Doula et al. (2009), KQ Vel would achieve its slow rotation after $\sim$ 200 Myr at a mass-loss rate of

$10^{-13} M_\odot$ yr$^{-1}$, while it would take $\sim 2$ Gyr at $10^{-15} M_\odot$ yr$^{-1}$. Kochukhov & Bagnulo (2006) estimated the age of KQ Vel as 260 Myr (assuming a single star evolution). If the secondary which we observe now as KQ Vel, was re-rejuvenated due to binary mass exchange or merger , it may be even younger. Hence we roughly assume $\dot{M} \sim 10^{-13} M_\odot$ yr$^{-1}$ as consistent with both the stellar age and spectral type of KQ Vel.

Assuming a NS accreting donor's stellar wind (Davidson & Ostriker 1973), the resulting X-ray luminosity of KQ Vel is $\sim 10^{27}$ erg s$^{-1}$, i.e. a few orders of magnitude below the observed. Furthermore, the strong magnetic field of KQ Vel dominates over its feeble stellar wind. As a result, the plasma-$\beta$ is very low (Altschuler & Newkirk 1969). Using equation (5) from Oskinova et al. (2011) and adopting as an upper limit on the wind speed 1000 km s$^{-1}$, we roughly estimate the *Alfvén* radius of KQ Vel as $> 150 R_*$ – well within the orbital separation of $245 R_*$. It means that only a small fraction of the wind ($\lesssim 1\%$) which consists of neutral hydrogen and metals can escape the stellar magnetosphere and feed the NS. Hence, we can rule out direct accretion onto a compact object as an explanation for the observed X-ray luminosity.

Some middle-age rotation powered pulsars can emit X-rays at the level we observe in KQ Vel (Becker & Truemper 1997; Kargaltsev et al. 2005). In this case, the pulsed X-ray emission modulated with a NS spin period of less than a dozen seconds is expected. Unfortunately, our *Chandra*'s data are not well suited to search for such pulsation. The X-ray spectra of KQ Vel are consistent with the presence of thermal optically thin plasma. This is quite different from the X-ray spectra of rotation powered pulsars. Hence, we believe that the current data do not support the presence of a middle aged pulsar in the KQ Vel system.

Among commonly detected Galactic X-ray sources are cataclysmic variables (CV) (e.g. Revnivtsev et al. 2006). These interacting binaries consist of an accreting white dwarf (WD) and a low-mass donor star filling its Roche lobe. CVs could have X-ray luminosities and hard X-ray spectra comparable with those observed in KQ Vel. Many CVs have relatively weak and broad emission lines in their spectra, which, combined with the CVs being much fainter than A stars, could potentially lead to an undetectable Ap+CV triple system[2].

This, however, meets difficulties given the vast difference in ages among A-type stars and typical CVs. The age of optical star in KQ Vel is $< 300$ Myr. At this age a WD may already be formed but generally CVs belong to much older stellar populations. The Ap star in the KQ Vel system could be a result of a merger, and hence being rejuvenated (see sect. 3.4). Nevertheless, even in this case, it would require a fine tuning to produce an AOV+CV system. Another consideration against a CV nature of the KQ Vel companion, is that some CVs are associated with novae. For such a bright (V=6.11 mag) and nearby star, a historical nova would have a good chance to be noticed if happen at the time of existing southern hemisphere records. However, since the typical recurrence time for classical novae is hundreds of years, a nova outburst associated with KQ Vel might have been missed. Therefore, while we currently do not favor the CV nature of the KQ Vel companion, this explanation cannot be ruled out.

### 3.3.2. Propelling neutron star

When a magnetized NS is embedded in stellar wind with very low mass-loss rate, such as in KQ Vel, the quasi-spherical sub-

---

[2] This possibility was suggested by the anonymous reviewer

sonic regime of accretion sets in (Shakura et al. 2012). The wind is gravitationally captured from a volume much larger than determined by the outer boundary of the corotating portion of the NS magnetosphere, $R_A$. Denote the characteristic radius of the volume from which material can be captured as $R_B$. In a rotating NS, the Keplerian radius is defined as $R_K = (GM_{NS}/\omega^2)^{1/3}$ with $\omega = 2\pi/P_{NS}$ for the NS spin period. If the condition $R_K \leq R_A$ is met, the accretion is throttled through the "propeller effect" (Illarionov & Sunyaev 1975). When the captured gas lacks the specific angular momentum to pass into the corotating magnetosphere, the accumulated wind material can form an extended, quasi-spherical envelope of hot, X-ray emitting gas.

In this situation, the NS is not accreting, and the captured stellar wind remains in the NS gravitational potential. The energy source preventing the gas from cooling is the mechanical power supplied by a propelling NS, which is mediated by the magnetic forces and convection in the shell. In this sense, the mass-loss from the optical star is not the parameter directly regulating the shell structure. Much more important (see Appendix) is the stellar wind velocity which determines the outer shell radius. The density at the shell base, $\rho_A$, is related to the total mass of the gas in the shell which determines the observed emission measure ($EM$) (using a crude analogy, the gas density near the ground on Earth is determined by the total mass and temperature of the Earth atmosphere). Therefore, there is no direct relation of $\rho_A$ with the poorly known stellar wind mass-loss rate. X-ray emission from the gas shell is sustained by the NS spin-down and not by wind accretion, hence the orbital eccentricity is irrelevant.

It is possible to obtain a self-consistent solution for the hot envelope using the parameters of KQ Vel. The detailed model calculations are described in the Appendix. We adopt the NS mass as $M_{NS} = 1.5 M_\odot$, and use constraints from the X-ray observations: $L_X \approx 2 \times 10^{30}$ erg s$^{-1}$, $EM \approx 5 \times 10^{52}$ cm$^{-3}$, $\bar{T} \approx 1$ keV (Table 2). Then, following the theory of quasi-spherical accretion, the derived inner and outer radii ($R_A$ and $R_B$), the mass of the shell $M_{sh}$, the wind speed of the A0p star, and the magnetic moment ($\mu$) of the NS are: $v_w \approx 500$ km s$^{-1}$, $R_A \approx 0.1 R_\odot$, $R_B \approx 2.2 R_\odot$, $\mu_{30} \approx 3$, $M_{sh} \approx 1 \times 10^{-14} M_\odot$, $\mu_{30} \approx 3$, where $\mu_{30}$ is the magnetic moment of the NS normalized to $10^{30}$ G cm$^3$ – a typical value for a NS.

The derived quantities are in good agreement with the expected properties of the KQ Vel system. The wind speed, 500 km s$^{-1}$, is appropriately realistic. The derived $R_A = 0.1 R_\odot$ implies if the NS has spin period $P_{NS} \lesssim 260$ s, it will be in a propeller state. Such spin period is quite reasonable for a NS that has not spun-down to the accretion stage, given the weak stellar wind of the A0p companion and a large binary separation.

While the accretion power is far too small to explain the observed X-ray luminosity of KQ Vel, the propelling NS injects significant amount of energy via interaction of the rotating magnetosphere and the matter in the shell. The maximum power which is provided by a propelling NS is $\approx 2\pi(\mu^2/R_A^3)/P_{NS}$ (Shakura et al. 2012). Inserting parameters derived for KQ Vel, the NS should have $P_{NS} \lesssim 100$ s, to explain the observed X-ray luminosity. According to the Eqs. (A.15) and (A.16), the NS spin-down can power the hot shell surrounding NS in the KQ Vel system at the present level for at least $10^5$ years.

Furthermore, the theory of quasi-spherical accretion naturally explains the variability seen in the X-ray light curve (Figs. 2). The time scale of observed X-ray variability, $P_X \sim 3000$ s, is much shorter than either the orbital period of the binary ($P_{orb} = 840$ d) or the spin period of the A0p star ($P_{rot} = 2800$ d). At the same time, it is at least an order of magnitude longer than

the predicted NS spin period, $P_{NS} \lesssim 100$ s. However, according to the Eq. (A.13), the free-fall time a hot convective shell surrounding the NS is $t_{ff} \simeq 3200$ s $(v_w/500 \text{ km s}^{-1})^{-3}$, i.e. very similar to the observed variability time scale in KQ Vel.

Finally, one should consider the special properties of KQ Vel, specifically the strong magnetic field of the donor star and hence its magnetized wind. The estimates show (see the Appendix) that the magnetic reconnection of the accretion flow and the NS field provides an important source of plasma heating maintaining the hot envelope around the NS in the KQ Vel binary system.

### 3.4. Evolutionary considerations: was KQ Vel a triple?

The KQ Vel system has a wide and eccentric orbit. If a NS is present in the system, a supernova (SN) must have occurred without disrupting the binary. In the absence of an additional kick velocity, the orbital eccentricity following the SN event would become $e = \Delta M/(M_{NS} + M_{opt})$. For the parameters of KQ Vel (Tab. 1), $\Delta M = 0.36 \cdot (3 + 1.5) = 1.6 \, M_\odot$. Hence, the NS progenitor mass can be roughly estimated as $1.6 + 1.5 \approx 3 \, M_\odot$. This likely was a He-star, stripped during the mass-exchange event. The initial mass of the NS progenitor can then be estimated (see Postnov & Yungelson 2014) as $M_{He} = 0.1 M_{init}^{1.4}$, or a total mass of $\sim 11 \, M_\odot$. Taking into account the long orbital period, the progenitor system might have been a C-type (i.e., a wide binary). In such cases the mass transfer can be highly unstable and likely non-conservative, and the hydrogen envelope will be lost without adding mass to the $3 \, M_\odot$ secondary companion. A sort of common envelope (CE) may have occurred, but the efficiency of CE in wide binaries is uncertain.

This alternative scenario may help to shed light on the origin of KQ Vel system and its peculiar properties, particularly the strongly magnetic nature of the optical star. It has long been believed, and recently confirmed by numerical modeling, that strongly magnetic massive stars result from stellar mergers (Schneider et al. 2019). In this case, KQ Vel was originally a triple system, where the present-day Ap star is the merger product, possibly of a W UMa type system. The NS is the tertiary remnant. If the initially less massive tertiary gained mass during the Roche lobe overflow by either of the primary binary components, the orbital separation would have increased.

The eccentric Kozai-Lidov mechanism (Naoz & Fabrycky 2014) operating in triple systems causes strong inclination and eccentricity fluctuations, and leads to the tightening of the inner binary. The merger product of the inner binary is observed today as the magnetic Ap star. The tertiary, with a mass in the range $8 - 10 \, M_\odot$ may have evolved to an electron-capture SN, without disrupting the system, and formed the NS we observe today.

The proximity of KQ Vel to Earth implies that the KQ Vel-like systems cannot be exotic and exceptionally rare. The lifetime of a propelling NS is $\sim 10^5 - 10^6$ yr, i.e. significantly less than a few $\times 10^8$ yr lifetime of an A0-type star. After the NS has spun down and the propeller stage has ended, the NS will enter the accretion regime, however given a very small accretion rate, its X-ray luminosity will be small (sect. 3.3.1). Given a large orbital separation, the binarity may be easily missed during a routine spectroscopic analysis. Future work on astrometric catalogs, e.g. *Gaia*, will be undoubtedly useful to shed more light on the population of wide intermediate mass binaries with X-ray dim NS companions.

## 4. Conclusions

*Chandra* X-ray observations of the strongly magnetic binary star KQ Vel revealed that its properties are exceptional for an Ap-type star: high X-ray luminosity, hard spectrum, and variable X-ray light-curve. The observed spectrum can be well fit either by a multi-temperature thermal plasma spectral model, or by a hybrid model consisting of thermal and a non-thermal emission components. We prefer the former spectral model, and explain the non-thermal component as being due to the auroral mechanism, i.e. similar to the Ap star CU Vir.

Exploring several different interpretations, we concluded that the theory of quasi-spherical accretion onto propelling NS with $P_{NS} \lesssim 100$ s and $\mu_{30} \approx 3$ best describes the hot plasma temperature, its emission measure, and the time scale of X-ray variability observed in KQ Vel. Thus, new X-ray *Chandra* observations strongly support the Bailey et al. (2015) suggestion on the presence of a compact companion in KQ Vel. We conclude that the compact companion is a NS in the propeller regime.

KQ Vel is the first known strongly magnetic Ap + NS binary. Confirmation of the existence of such objects has important consequences for our understanding of binary evolution and accretion physics.

## References

Altschuler, M. D. & Newkirk, G. 1969, Sol. Phys., 9, 131
Arnaud, K. A. 1996, in Astronomical Society of the Pacific Conference Series, Vol. 101, Astronomical Data Analysis Software and Systems V, ed. G. H. Jacoby & J. Barnes, 17–+
Asplund, M., Grevesse, N., Sauval, A. J., & Scott, P. 2009, ARA&A, 47, 481
Babel, J. 1996, A&A, 309, 867
Babel, J. & Montmerle, T. 1997, A&A, 323, 121
Bailey, J. D., Grunhut, J., & Landstreet, J. D. 2015, A&A, 575, A115
Becker, W. & Truemper, J. 1997, A&A, 326, 682
Borra, E. F. & Landstreet, J. D. 1975, PASP, 87, 961
Brown, J. C. 1971, Sol. Phys., 18, 489
Cowie, L. L., McKee, C. F., & Ostriker, J. P. 1981, ApJ, 247, 908
Davidson, K. & Ostriker, J. P. 1973, ApJ, 179, 585
Dempsey, R. C., Linsky, J. L., Fleming, T. A., & Schmitt, J. H. M. M. 1993, ApJS, 86, 599
Ducati, J. R., Bevilacqua, C. M., Rembold, S. r. B., & Ribeiro, D. 2001, ApJ, 558, 309
Fitzgerald, M. P. 1970, A&A, 4, 234
Han, Z., Podsiadlowski, P., Maxted, P. F. L., & Marsh, T. R. 2003, MNRAS, 341, 669
Horne, J. H. & Baliunas, S. L. 1986, ApJ, 302, 757
Huenemoerder, D. P., Phillips, K. J. H., Sylwester, J., & Sylwester, B. 2013, ApJ, 768, 135
Illarionov, A. F. & Sunyaev, R. A. 1975, A&A, 39, 185
Jaschek, M. & Jaschek, C. 1959, PASP, 71, 48
Kargaltsev, O. Y., Pavlov, G. G., Zavlin, V. E., & Romani, R. W. 2005, ApJ, 625, 307
Kochukhov, O. & Bagnulo, S. 2006, A&A, 450, 763
Kochukhov, O., Lüftinger, T., Neiner, C., Alecian, E., & MiMeS Collaboration. 2014, A&A, 565, A83
Krtička, J., Mikulášek, Z., Henry, G. W., et al. 2019, A&A, 625, A34
Leto, P., Trigilio, C., Leone, F., et al. 2020, MNRAS, 493, 4657
Leto, P., Trigilio, C., Oskinova, L., et al. 2017, MNRAS, 467, 2820
Leto, P., Trigilio, C., Oskinova, L. M., et al. 2018, MNRAS, 476, 562
Mathys, G. 2017, A&A, 601, A14
Mereghetti, S. & La Palombara, N. 2016, Advances in Space Research, 58, 809
Montes, D., Fernandez-Figueroa, M. J., de Castro, E., & Cornide, M. 1995, A&A, 294, 165

Naoz, S. & Fabrycky, D. C. 2014, ApJ, 793, 137

Oskinova, L. M., Todt, H., Ignace, R., et al. 2011, MNRAS, 416, 1456

Postnov, K., Oskinova, L., & Torrejón, J. M. 2017, MNRAS, 465, L119

Postnov, K. A. & Yungelson, L. R. 2014, Living Reviews in Relativity, 17, 3

Prinja, R. K. 1989, MNRAS, 241, 721

Raymond, J. C., Cox, D. P., & Smith, B. W. 1976, ApJ, 204, 290

Revnivtsev, M., Sazonov, S., Gilfanov, M., Churazov, E., & Sunyaev, R. 2006, A&A, 452, 169

Robrade, J. 2016, Advances in Space Research, 58, 727

Robrade, J., Oskinova, L. M., Schmitt, J. H. M. M., Leto, P., & Trigilio, C. 2018, A&A, 619, A33

Schneider, F. R. N., Ohlmann, S. T., Podsiadlowski, P., et al. 2019, Nature, 574, 211

Schröder, C. & Schmitt, J. H. M. M. 2007, A&A, 475, 677

Shakura, N., Postnov, K., Kochetkova, A., & Hjalmarsdotter, L. 2012, MNRAS, 420, 216

Syunyaev, R. A. & Shakura, N. I. 1977, Soviet Astronomy Letters, 3, 138

Testa, P., Drake, J. J., Peres, G., & DeLuca, E. E. 2004, ApJ, 609, L79

Ud-Doula, A., Owocki, S. P., & Townsend, R. H. D. 2009, MNRAS, 392, 1022

Walter, F. M. & Bowyer, S. 1981, ApJ, 245, 671

## Appendix A: X-ray emission from a hot shell around a propelling neutron star in settling accretion regime

The X-ray emission properties from a hot shell around the magnetosphere of a propelling neutron star (a model applied to the $\gamma$ Cas phenomenon) were calculated in Postnov et al. (2017) (see Eqs. (2)-(11) in that paper). The calculations were carried out for the case of thermal bremsstrahlung cooling, which is valid for high plasma temperatures $kT \gtrsim 4$ keV. At lower plasma temperatures, the collisional cooling function becomes dominant, rapidly increasing down to temperatures $\sim 0.01$ keV. To estimate the properties of the shell in the temperature range $0.01 < kT < 4$ keV, we can use the analytical approximation for a fully ionized plasma with solar abundances (Raymond et al. 1976; Cowie et al. 1981):

$$\Lambda = K_{\rm cool}\, T^{-0.6}, \tag{A.1}$$

with $K_{\rm cool} = 6.2 \times 10^{-19}$ in cgs units. Below we shall replace the numerical power 0.6 with 3/5.

The total X-ray luminosity from an optically thin spherical shell located between the magnetospheric radius $R_{\rm A}$ and the outer radius $R_{\rm B}$ is

$$L_{\rm X} = \int\limits_{R_{\rm A}}^{R_{\rm B}} n_e^2\, \Lambda\, 4\pi\, r^2\, dr\,. \tag{A.2}$$

Here we have assumed a completely ionized H gas, with $n_{\rm H} = n_{\rm e} = \rho/m_{\rm H}$. For the outer boundary in the integral (A.2), we assume the Bondi radius with $R_{\rm B} = 2GM_{\rm NS}/v_{\rm w}^2$, where $M_{\rm NS}$ is the NS mass, $v_{\rm w}$ is the velocity of the wind from the optical star, and neglecting the orbital motion of the NS.

The density and temperature profiles in quasi-stationary gas envelope surround the NS magnetosphere (Shakura et al. 2012) are:

$$\rho(r) = \rho_{\rm A} \left(\frac{R_{\rm A}}{r}\right)^{3/2}, \text{ and} \tag{A.3}$$

$$T(r) = T_{\rm A} \left(\frac{R_{\rm A}}{r}\right). \tag{A.4}$$

Using the virial temperature of a monoatomic gas at the base of the shell $T_{\rm A} = GM_{\rm NS}m_{\rm H}/5kR_{\rm A}$, we obtain

$$L_{\rm X} = 4\pi \frac{5}{3} K_{\rm cool} \left(\frac{\rho_{\rm A}}{m_{\rm H}}\right)^2 R_{\rm A}^3 \left(\frac{GM_{\rm NS}m_{\rm H}}{5kR_{\rm B}}\right)^{-3/5} \left[1 - \left(\frac{R_{\rm A}}{R_{\rm B}}\right)^{3/5}\right]. \tag{A.5}$$

An important difference of Eq. (A.5) from the analogous Eq. (6) in Postnov et al. (2017) is that, due to inverse power-law temperature dependence of $\Lambda$, the X-ray luminosity is almost fully determined by the combination $\rho_{\rm A}^2 R_{\rm A}^3$ and the stellar wind velocity $v_{\rm w}$ (which sets the Bondi radius via $GM_{\rm NS}/R_{\rm B} = 1/2v_{\rm w}^2$). The ratio $R_{\rm A}/R_{\rm B}$ is typically $\ll 1$, which enables us to omit the second term in the square brackets in Eq. A.5. The $EM$ in the shell becomes:

$$EM = \int\limits_{R_{\rm A}}^{R_{\rm B}} n_{\rm e}^2 4\pi r^2 dr = 4\pi \left(\frac{\rho_{\rm A}}{m_{\rm H}}\right)^2 R_{\rm A}^3 \ln(R_{\rm B}/R_{\rm A})$$
$$= \frac{3}{5K_{\rm cool}} L_{\rm X} \left(\frac{GM_{\rm NS}m_{\rm H}}{5kR_{\rm B}}\right)^{3/5} \ln(R_{\rm B}/R_{\rm A})\,. \tag{A.6}$$

Noting that $GM_{\rm NS}/R_{\rm B} = v_{\rm w}^2/2$ and substituting the characteristic values $M_{\rm NS} = 1.5M_\odot$, $v_{\rm w} = 10^8$ cm s$^{-1} \times v_8$, $L_{\rm X} = 10^{30}$ erg s$^{-1} \times L_{30}$, we arrive at

$$EM \approx 1.15 \times 10^{52} L_{30}\, v_8^{6/5}\, \ln(R_{\rm B}/R_{\rm A})\ {\rm cm}^{-3}. \tag{A.7}$$

The logarithmic factor here is usually on the order of 3–4. The $EM$ is observationally constrained, hence it is possible to determine the mass contained in the shell, with

$$M_{\rm sh} = m_{\rm H} \int\limits_{R_{\rm A}}^{R_{\rm B}} 4\pi\, r^2\, n_{\rm H}(r)\, dr = \frac{8\pi}{3}\, m_{\rm H}\, n_{\rm A}\, R_{\rm A}^3\, (R_{\rm B}/R_{\rm A})^{3/2}. \tag{A.8}$$

Using Eq. A.5, and the density and temperature profiles in the shell, it is straightforward to derive the expression for the magnetospheric radius $R_{\rm A}$:

$$R_{\rm A} = \left(\frac{20\, K_{\rm cool}}{m_{\rm H}^2}\right)^{1/7} \left(\frac{5K_2}{2\pi}\right)^{2/7} \left(\frac{\mu^4}{L_{\rm X}}\right)^{1/7} \left(\frac{G M_{\rm NS}\, m_{\rm H}}{5k R_{\rm B}}\right)^{-3/35}$$
$$\simeq 4 \times 10^9\, \mu_{30}^{4/7} L_{30}^{-1/7} v_8^{-6/35}\ {\rm cm}. \tag{A.9}$$

Here $\mu = 10^{30}$ G cm$^3\, \mu_{30}$ is the NS magnetic moment, $K_2 \approx 7.7$ is a numerical factor that takes into account the difference of the NS magnetosphere from a pure dipole shape (c.f., Shakura et al. (2012)). For typical wind velocities, $R_{\rm B} \sim 4 \times 10^{10}\, v_8^{-2}$ cm, and therefore our assumption $R_{\rm B}/R_{\rm A} \gg 1$ is justified.

The temperature at the base of the shell is $T_{\rm A} \propto R_{\rm A}^{-1} \simeq 10$ keV $\mu_{30}^{-4/7} L_{30}^{1/7} v_8^{6/35}$. However, relevant to the fit of the observed spectrum is neither the maximum nor the minimum temperature, but the average temperature as weighted by $EM$. The predicted average temperature, $\bar{T}$, is given by

$$\bar{T} = \frac{\int_{T_{\rm A}}^{T_{\rm B}} T(r)\, dEM}{\int_{T_{\rm A}}^{T_{\rm B}} dEM}. \tag{A.10}$$

With $dEM = n^2(r)\, 4\pi\, r^2\, dr$, and using the preceding expressions, along with $R_{\rm B} \gg R_{\rm A}$, the weighted average temperature becomes

$$\bar{T} \approx \frac{T_{\rm A}}{\ln(R_{\rm B}/R_{\rm A})}. \tag{A.11}$$

Given that the denominator is typically of order a few, the characteristic thermal temperature expected from the hot shell model is a factor of a few smaller than the temperature at the inner boundary of the shell.

Related to spectral fitting is the column density distribution of material in the shell. Even if hydrogen is completely ionized in the hot shell, it is standard to express the column as $N_{\rm H}$. Much of the absorption at the higher energies derives from photoabsorption by metals. Along a radial through the annual shell and assuming $R_B/R_A \gg 1$, the column density is:

$$N_{\rm H} = \int\limits_{R_{\rm A}}^{R_{\rm B}} n_{\rm H}(r)\, dr \simeq 2R_{\rm A}\rho_{\rm A}/m_{\rm H} \tag{A.12}$$

Equations (A.5, A.6, A.11) enable us to express three independent model parameters, $\rho_{\rm A}$, $R_{\rm A}$ and $R_{\rm B}$ (or $v_{\rm w}$) through the values which are directly derived from observations: $L_{\rm X}$, $EM$,

and $\bar{T}$. Then, Eq. A.9 can be used to estimate the NS magnetic field.

Finally, let us check whether the shell can remain hot under assumed form of the cooling function that increases along the radius as $\Lambda \sim T^{-0.6} \sim r^{0.6}$. The free-fall time of the hot envelope is given by

$$
t_{\mathrm{ff}} = \frac{R_{\mathrm{B}}^{3/2}}{\sqrt{2\,G\,M_{\mathrm{NS}}}} = \frac{2\,G\,M_{\mathrm{NS}}}{v_{\mathrm{w}}^3} \simeq 3200 \text{ s } (v_{\mathrm{w}}/500 \text{ km s}^{-1})^{-3}.
$$
(A.13)

The plasma cooling time in the isentropic shell can be expressed as

$$
t_{\mathrm{cool}}(r) = \frac{3kT}{n_e\Lambda} \simeq 10^3[\mathrm{s}]\frac{T_A^{8/5}(R_A/r)^{8/5}}{n_a(R_A/r)^{3/2}}
$$
$$
= 10^3[\mathrm{s}]\left(\frac{R_A}{r}\right)^{1/10}\left[\frac{\ln(R_B/R_A)}{3}\right]^{1/2}\left(\frac{EM}{5\times10^{52}\text{ cm}^{-3}}\right)^{-1/2}
$$
(A.14)

which is almost constant across the shell. However, this time is dangerously close to the free-fall time $t_{\mathrm{ff}} \sim 3 \times 10^3[\mathrm{s}](r/R_{\mathrm{B}})^{3/2}$. This suggests that if there were no additional plasma heating in the shell, the captured gas would rapidly cool below $R_{\mathrm{B}}$ to form a cold dense 'dead' disk around the magnetosphere (Syunyaev & Shakura 1977), and no hot convective shell would be formed.

Luckily, in the case of magnetized wind the magnetic reconnection can heat up plasma. Indeed, the reconnection time in a magnetized plasma blob of size $l$, mass $m_{\mathrm{b}} \sim \rho_{\mathrm{b}}l^3$ and magnetic field $B_{\mathrm{b}}$ can be written as $t_{\mathrm{r}} \sim l/v_{\mathrm{r}}$, where $v_{\mathrm{r}}$ is the reconnection rate scaling as the Alfvén velocity $v_A \sim B_{\mathrm{b}}/\sqrt{\rho_{\mathrm{b}}}$. Therefore, $t_{\mathrm{r}} \sim l\sqrt{\rho_{\mathrm{b}}}/B_{\mathrm{b}}$, and using the magnetic flux conservation $B_{\mathrm{b}}^2 = const$ we arrive at $t_{\mathrm{r}} \sim l^3\sqrt{\rho_{\mathrm{b}}} \sim m_{\mathrm{b}}/\sqrt{\rho_{\mathrm{b}}}$. The magnetic reconnection heating is effective if $t_{\mathrm{r}}/t_{\mathrm{cool}} \sim (m_{\mathrm{b}}\rho)/T_{\mathrm{b}}^{8/5} < 1$. By neglecting mass decrease of the falling blob (due to, for example, Kelvin-Helmholtz stripping), assuming the adiabatic blob evolution (i.e. $\rho_{\mathrm{b}}T_{\mathrm{b}}l^{5/3} = const$) in the surrounding plasma with pressure $P_e \sim n_eT_e$ and pressure balance $P_{\mathrm{b}} \sim \rho_{\mathrm{b}}T_{\mathrm{b}} = P_e$, we arrive at $t_{\mathrm{r}}/t_{\mathrm{cool}} \propto r^{\frac{189}{20}}$ (here the adiabatic scaling for the surrounding plasma density and temperature, Eqs. (A.3) and (A.4), were applied). This means that the magnetic reconnection in freely falling magnetized plasma blobs can rapidly occur providing additional heat sustaining the hot convective shell. On top of the plasma heating, the magnetic blob reconnection results in the generation of a $\sim 10\%$ non-thermal tail. Realistically, not all free-falling blobs are magnetized, and part of them can cool down thus increasing $N_{\mathrm{H}}$ relative to the hot plasma estimate Eq. (A.12) above.

The spin-down timescale of the propelling NS is

$$
t_{\mathrm{sd}} = \omega_{\mathrm{NS}}/\dot{\omega}_{\mathrm{NS}} = (I\omega_{\mathrm{NS}}^2/L_{\mathrm{X}})(1 + \epsilon),
$$
(A.15)

where $I$ is the NS moment of inertia, and $\epsilon = L_{\mathrm{mr}}/L_{\mathrm{sd}}$ is the ratio of the NS spin-down power, $I\omega_{\mathrm{NS}}\dot{\omega}_{\mathrm{NS}}$, to the power supplied by magnetic reconnection. Then

$$
t_{\mathrm{sd}} \simeq 2 \times 10^5[\mathrm{yrs}]\left(\frac{P_{\mathrm{NS}}}{100\text{ s}}\right)^{-2}\left(\frac{L_{\mathrm{X}}}{10^{30}\text{ erg s}^{-1}}\right)(1 + \epsilon).
$$
(A.16)